

## A dual-wavelength interrogation schema for trace gas photoacoustic spectroscopy

Ji Yan<sup>1</sup>, Yi Ying-Yan<sup>1</sup>, Li Min<sup>1\*</sup>, Lu Hai-Fei<sup>1</sup>, Wen Xiao-Yan<sup>1</sup>, Li Yu-Lin<sup>2</sup>

(1. Department of Physics, Wuhan University of Technology, Wuhan 430070, China;  
2. Wuhan Jingyu Electro-Optic Technology Company Limited, Wuhan 430070, China)

**Abstract:** Photoacoustic spectroscopy is the most sensitive approach of trace gas analysis reaching part per trillion by volume level and available for engineering practice, but not sufficiently satisfy the measurement demand of gases with weak absorption in near infrared zone. This paper presents a simple interrogation method using a dual-wavelength schema to switch effectively between the absorption and unabsorption lines of the gas to be measured, which takes good advantage of the current modulation characteristic of laser diode. Measurement results of methane demonstrate the feasibility and a relatively simple way to reach resolution of 0.46 ppm of the dual-wavelength method when the laser power is 2.1 mW.

**Key words:** photoacoustic spectroscopy, dual-wavelength schema, current modulation

**PACS:** 42.55.Px, 42.60.Fc

## 基于双波长法的光声光谱气体检测

季焱<sup>1</sup>, 易迎彦<sup>1</sup>, 黎敏<sup>1\*</sup>, 吕海飞<sup>1</sup>, 文晓艳<sup>1</sup>, 李玉林<sup>2</sup>

(1. 武汉理工大学理学院物理系, 湖北 武汉 430070;  
2. 武汉精昱光电科技有限公司, 湖北 武汉 430070)

**摘要:**光声光谱法是检测气体最灵敏的方法, 气体浓度检测精度可达到 ppt 量级, 但这需要复杂的实验系统和昂贵的器材, 不利于在工程实践上使用. 本文基于可调激光器的电流调制特性, 提出了一种在测量气体吸收谱的吸收零点和吸收峰之间有效切换波长的简单调制方法. 当激光功率为 2.1 mW 时, 甲烷气体浓度的测量极限可达到 0.46 ppm, 测量结果证明了双波长法的可行性.

**关键词:**光声光谱; 双波长法; 电流调制

中图分类号: O433.4 文献标识码: A

## Introduction

Photoacoustic spectroscopy (PAS) is characterized by fast response, over-all high selectivity and sensitivity. It is the most versatile method for trace gas analysis<sup>[1-2]</sup>. Since photoacoustic (PA) cell is only in resonance with the incident light pulse at a specific frequency that matches the length of the resonant cell, the modulation method of the light source has great influence on the capability of the PAS based sensing system. Laser diode (LD) has considerable merit of direct current modulation. High power LDs push the concentration sensitivity

of PA gas detection into part per trillion by volume (ppt) level or even below<sup>[3-4]</sup> which has promoted the industrialization of photoacoustic devices.

In recent years, in order to improve the signal-to-noise ratio (SNR) of the PAS system, major researches have focused on novel designs of PA cell and acoustic signal processing technology. The optimizations of PA cells have been presented in two main categories: (1) using highly sensitive acoustic sensors, such as quartz-enhanced PAS<sup>[5]</sup> and cantilever-enhanced PAS<sup>[6]</sup>, (2) using high performance PA cell for trace gas analysis and detection<sup>[7-8]</sup>. Compared with electronic microphone, quartz tuning fork and cantilever microphone show obvi-

**Received date:** 2017-09-29, **revised date:** 2018-01-16

**收稿日期:** 2017-09-29, **修回日期:** 2018-01-16

**Foundation items:** Supported by National Natural Science Foundation of China (NSFC 61307099), the Fundamental Research Funds for Central Universities (WUT 2016-IA-009)

**Biography:** Ji Yan (1992-), male, Wuhan China, master. Research fields focuses on optical sensing and gas detection. E-mail: 15370932898@163.com

\* **Corresponding author:** E-mail: minli@whut.edu.cn

ous advantages in sensitivity and dynamic range, while making the PA cell more complicated. High-performance PA cells which could offer high cell constant of more than  $3000 \text{ Pa} \cdot \text{cm}/\text{W}$ , high magnification of 100 times or low external noise, require ideal materials and exquisite technique which are even harder to realize. Efforts to optimize signal processing technologies have also been presented in two categories: (1) using reference PA cell to suppress background signal, (2) using various digital signal processing methods to extract the effective signal from noise<sup>[9-10]</sup>. Reference PA cell complicates and increases the system cost for the additional measurement unit or mechanical adapters. On the other hand, digital signal processing methods such as wavelet analysis or duffing oscillator may not effectively improve the SNR of the PAS system based on poor original signal. Neither a complex PA cell nor a signal processing system is conducive to the popularity of PAS.

In this paper, a new dual-wavelength interrogation method is proposed to improve the SNR of PAS sensing system by taking advantage of the convenient wavelength modulation of LDs. Measurement results of methane ( $\text{CH}_4$ ) demonstrate the feasibility and improvement of SNR of the dual wavelength interrogation method.

## 1 Dual-wavelength interrogation for photoacoustic spectroscopy

PA signal only generates when the central wavelength of light source matches the absorption line of the gas to be measured in the PA cell, where light is absorbed and transmitted into gas molecular movement. When the light source is periodically modulated at the resonance frequency of the PA cell, the amplified acoustic wave is easily picked up by a sensitive microphone. The linewidth of the gas absorption peak is about  $0.1 \text{ nm}$  in the near infrared zone, 10 times of that of distributed feedback LD (DFB-LD). The operating wavelength of DFB-LD is conveniently shifted  $\pm 0.5 \text{ nm}$  away from the setting working point at specific temperature by directly changing the driving current, which means we might measure the PA signals at two different wavelengths by simply applying a frequency modulation signal to the driving current of the DFB-LD. If the modulation depth is deep enough, the central wavelength of DFB-LD switches between the absorption peak of the measured gas and more than  $0.1 \text{ nm}$  away from the absorption peak, which is very similar to on-off states of gas absorption and named as dual-wavelength interrogation (DWI) method.

## 2 Experiments and discussion

The main parts of our complete photoacoustic system are shown schematically in Fig. 1. The excited sound wave was detected by a condenser microphone (Knowles, WP-23502) with a responsivity of  $25 \text{ mV}/\text{Pa}$ . The output signal of microphone passed the filter amplifier circuit with  $10^4$  times amplification and was finally processed by a processor. The PA cell consists of a central cylindrical acoustic resonator (diameter =  $4.5 \text{ mm}$ , length =  $60 \text{ mm}$ ) and two buffer volumes (diameter =  $17 \text{ mm}$ , length =  $30 \text{ mm}$ ). Figure 2 shows the frequen-

cy spectrum of the PA cell in a range of  $2400 \text{ Hz}$  to  $3300 \text{ Hz}$  under an acoustic pressure of  $0.1 \text{ Pa}$ . A dominant resonance peak at about  $2840 \text{ Hz}$  is clearly shown.

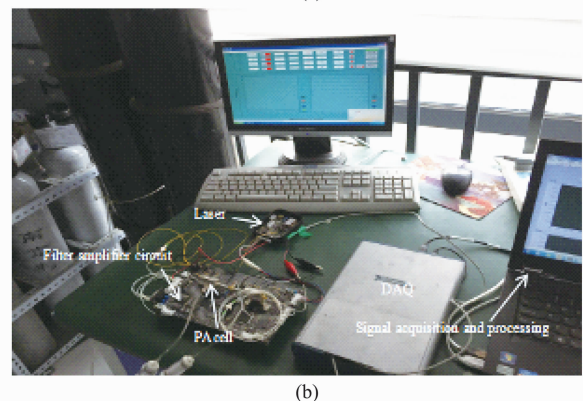
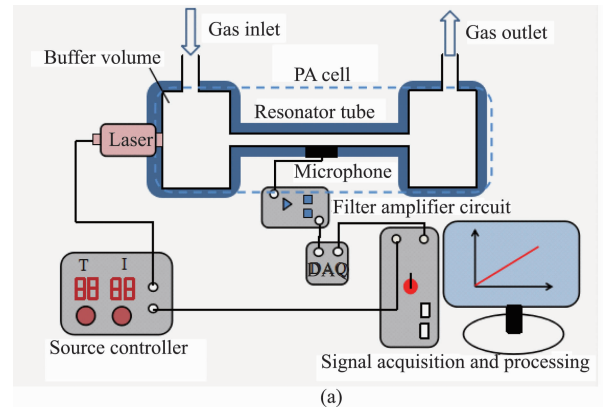


Fig. 1 (a) Photoacoustic gas detection system, (b) photo of the system

图 1 (a) 光声气体检测系统, (b) 系统实际图

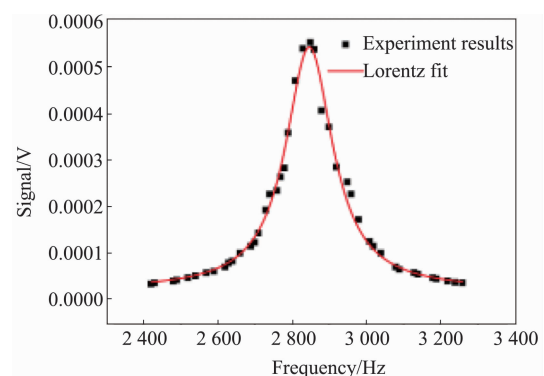


Fig. 2 The responding spectrum of the  $\text{CH}_4$  measurement system

图 2 甲烷测量系统的频谱响应

The  $\lambda_0$  was set to  $1653.72 \text{ nm}$ , and the variation range of  $\lambda$  was from  $1653.72 \text{ nm}$  to  $1653.25 \text{ nm}$ , larger than the full width half maximum (FWHM) of the  $\text{CH}_4$  absorption curve of  $0.04 \text{ nm}$ . The PA signals were measured with  $2010 \text{ ppm}$   $\text{CH}_4$  with  $\text{N}_2$  as the accompanying gas only. As  $\lambda$  shifts to shorter wavelength, the wavelength difference increases while the corresponding ab-

sorption coefficient of  $\text{CH}_4$  decreases. The responding PA signal climbs up dramatically before the turning point when  $\lambda$  moves completely outside of the FWHM of  $\lambda_0$ , then it becomes flatten. The downwards trend in Fig. 3 is caused by capacitors in the control circuit of the laser, whose charge-discharge characteristics always cause interrogation waveform distortion. The greater the modulation depth is, the longer the current interrogation lasts, and the more serious the waveform distortion is.

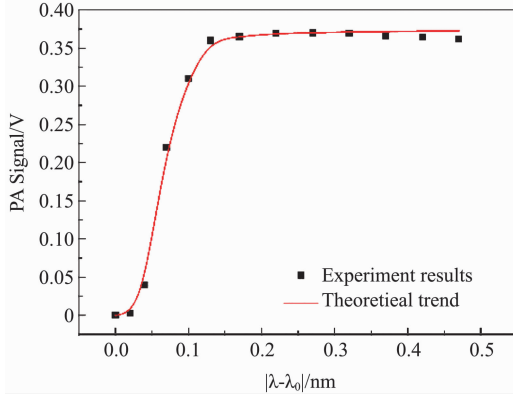


Fig. 3 Relationship between the  $|\lambda-\lambda_0|$  and the PA signal  
图3 调制深度  $|\lambda-\lambda_0|$  与光声信号的关系

The response of the PA signal amplitude to  $\text{CH}_4$  concentration was measured and plotted in Fig. 4. Specific values are shown in Table 1. A linearity of 0.99 has been obtained in the concentration range from 10 to 2010 ppm. We applied three typical waveforms, i. e., square, triangle and sine wave to the driving current of the DFB-LD with a modulation depth of 10%, which set  $\lambda$  to 1 653. 6 nm. The output signal modulated with square wave was proved to gain the best response, about 1. 1 and 2. 1 times of the signal amplitude modulated with sine wave and triangle wave, respectively. Similarly, the slope of the square wave modulation was the greatest, which indicated that the square wave modulation DWI-PA system has the best sensitivity.

**Table 1 The PA signal response to the  $\text{CH}_4$  concentration (LD output power at 2. 1mW,  $\lambda_0$  and  $\lambda$  as 1653. 72 nm and 1653. 6 nm, respectively)**

表1 不同浓度对应的光声信号: 光源输出功率为 2. 1 mW,  $\lambda_0$  和  $\lambda$  分别设置为 1653. 72 nm 和 1653. 6 nm

Concentration/ppm	Square wave/mV	Sine wave/mV	Triangle wave/mV
10. 6	8. 1	2. 6	1. 2
57. 3	14. 5	7. 4	6. 4
335	62	41. 2	29. 1
502	100. 1	57. 2	40. 5
1005	183. 4	119. 9	89. 3
2010	377. 8	228. 5	180. 2

The detection limit of the system is written as:

$$C_{\min} = \frac{c}{\text{SNR}}, \quad (1)$$

where  $C_{\min}$  and  $c$  are the minimum detection limit of the

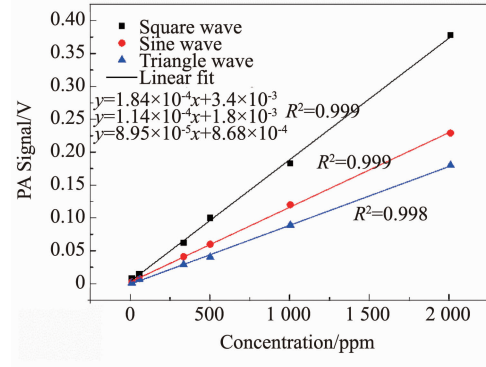


Fig. 4 Calibration curve for  $\text{CH}_4$   
图4 甲烷浓度与光声信号的关系曲线

system and the gas concentration. The system sensitivity is obtained by calibrating using standard gases. As concentration and corresponding SNR are already known, the sensitivity of the system was obtained directly using Eq. (1). The minimum detection limit of the DWI-PA system can be deduced using the data in Table 2 with concentration of 10. 6 ppm. The detection limits for  $\text{CH}_4$  gas were 0. 46, 1. 43, and 3. 09 ppm with square, triangle and sine wave modulation, respectively. There are several possibilities to lower the detection limit. A reduction of noise can be achieved by using sound insulation outside the device. Further improvements can be made by optimizing the PA cell dimensions for the source in order to minimize the background signals from the walls and windows.

**Table 2 Mean values of signal and noise (LD output power at 2. 1 mW, 10. 6 ppm of  $\text{CH}_4$  with  $\text{N}_2$  as the background)**

表2 光声信号与噪声信号的平均值: 光源输出功率为 2. 1 mW,  $\text{N}_2$  为背景气体,  $\text{CH}_4$  浓度为 10. 6 ppm

Modulating waveforms	Square wave	Sine wave	Triangle wave
PA signal/mV	8. 1	2. 6	1. 2
Noise/mV		0. 35	
$C_{\min}$ /ppm	0. 46	1. 43	3. 09

Figure 5 shows the interrogation signals of different waveforms in the  $\text{CH}_4$  measurement system. In a complete cycle, the effective area of square wave in the gas absorption spectrum is greater than that of the sine wave. The gas in the PA cell absorbs more light, and the pressure difference after the release of heat is greater. Similarly, the PA signal interrogates with sine wave is larger than that with triangular wave. Thus, under the same experimental conditions, the PA signal interrogates with square wave is larger than that with the sine wave and the triangle wave. When the wavelength  $\lambda$  deviates from  $\lambda_0$ , the corresponding absorption coefficient decreases rapidly, then it becomes flat. The pressure difference caused by light absorbing and heat releasing in the PA cell gradually increases. Thus, the PA signal interrogating with square wave increases rapidly before becoming flat. On the other hand, the effective area of the sine wave or triangular wave within the absorption spectrum increases in

the first half period then decreases in the second half. Thus, the PA signal interrogates with sine wave or triangle wave increases first then decreases with the energy variation. The results of different modulation waveforms are shown in Fig. 6, where theoretical parameters of  $P$ ,  $C_{\text{cell}}$ , and  $S_m$  are applied, and  $c$  is set to 10 ppm.

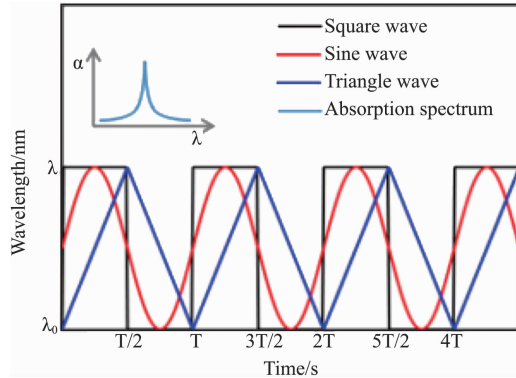


Fig. 5 Interrogation waveforms  
图5 调制波形

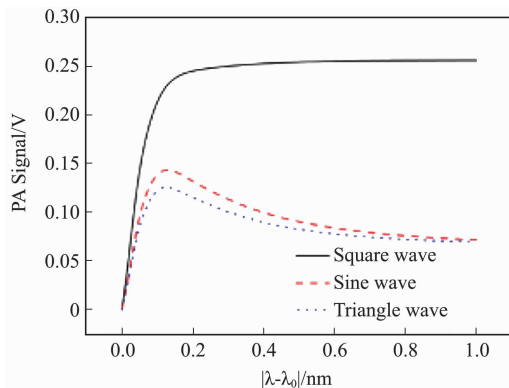


Fig. 6 The response of PA signal to the  $|\lambda - \lambda_0|$   
图6 光声信号与调制深度 $|\lambda - \lambda_0|$ 的对应关系

### 3 Conclusion

This paper presents a simple interrogation method

using a dual-wavelength schema, which takes good advantage of the current interrogation characteristic of laser diode. The appropriate dual-wavelength setting can effectively increase the amplitude of the PA signal and improve the SNR. Compared with sine wave and triangle wave, square wave interrogation produces greater PA signals. Measurement results of  $\text{CH}_4$  demonstrate the feasibility and simplicity of the dual-wavelength method which could reach resolution of 0.46 ppm when the laser power is 2.1 mW.

### References

- [1] Martin P A. Near-infrared diode laser spectroscopy in chemical process and environmental air monitoring [J]. *Chemical Society Reviews*, 2002, **31**(4):201-10.
- [2] Schilt S, Thévenaz L, Niklès M, et al. Ammonia monitoring at trace level using photoacoustic spectroscopy in industrial and environmental applications[J]. *Spectrochimica Acta Part A Molecular & Biomolecular Spectroscopy*, 2004, **60**(14):3259.
- [3] Yin X K, Dong L, Wu H P, et al. Sub-ppb nitrogen dioxide detection with a large linear dynamic range by use of a differential photoacoustic cell and a 3.5 W blue multimode diode laser[J]. *Sensors and Actuators B: Chemical*, 2017, **247**:329-335.
- [4] Yi H, Liu K, Chen W, et al. Application of a broadband blue laser diode to trace  $\text{NO}_2$  detection using off-beam quartz-enhanced photoacoustic spectroscopy[J]. *Optics Letters*, 2011, **36**(4):481.
- [5] Yi H, Chen W, Vicet A, et al. T-shape microresonator-based quartz-enhanced photoacoustic spectroscopy for ambient methane monitoring using 3.38- $\mu\text{m}$  antimonide-distributed feedback laser diode [J]. *Applied Physics B*, 2014, **116**(2):423-428.
- [6] Koskinen V, Fonsen J, Roth K, et al. Progress in cantilever enhanced photoacoustic spectroscopy [J]. *Vibrational Spectroscopy*, 2008, **48**(1):16-21.
- [7] Gondal M A, Dastageer A, Shwehdi M H. Photoacoustic spectrometry for trace gas analysis and leak detection using different cell geometries [J]. *Talanta*, 2004, **62**(1):131-14.
- [8] Starecki T, Geras A. Improved open photoacoustic Helmholtz cell[J]. *International Journal of Thermophysics*, 2014, **35**(11):2023-2031.
- [9] Li J, Chen C, Zheng C, et al. Extraction of physical parameters from photoacoustic spectroscopy using wavelet transform[J]. *Journal of Applied Physics*, 2011, **109**(6):041101-469.
- [10] Li Y, Yang B J, Yuan Y, et al. Analysis of a kind of Duffing oscillator system used to detect weak signals[J]. *Chinese Physics B*, 2007, **16**(4):1072-1076.